

An Introduction to the Thermal Modelling and Characterisation of Semiconductor Bolometers

Matt Hollister

March 27, 2006

1 Introduction

In modern astronomy, bolometers are the best choice of detector for radiation at wavelengths between $200\ \mu\text{m}$ and $3\ \text{mm}$. At shorter wavelengths, detection of radiation is possible by direct excitation of charge carriers, while at longer wavelengths, heterodyne systems win out over bolometric detectors. A bolometer is essentially a thermometer - the energy of an incoming photon is dissipated in an absorbing material, and the resultant temperature rise is measured as a change in voltage or current in the readout circuit. Modern semiconductor bolometers, such as the device shown in figure 1 from the SCUBA instrument, are of a “composite” construction in which the absorber and thermistor are separated, allowing the two elements to be optimised independently. Holland *et al.* provide a good overview of bolometer behaviour and usage.

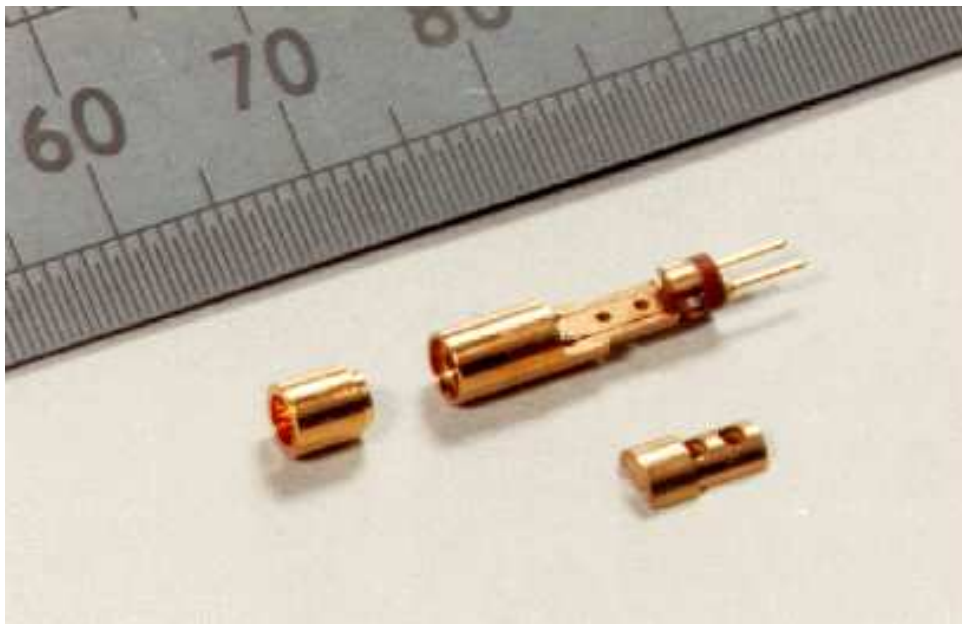


Figure 1: Composite bolometer from the SCUBA instrument.

In order to understand how a bolometer responds to absorbed radiation, we must be able to model the thermal behaviour of the detector, specifically how the electrical properties of the detector change with temperature and absorbed power. This seminar aims to provide an introduction to the principles of bolometer characterisation by describing a model for an ideal bolometer, and how we can fit that model to experimental data to understand the device we are measuring.

2 Bolometer Thermal Model

Figure 2 shows a schematic of a simple bolometer model. Regardless of the geometry of the device, all such detectors can be described in this way. A bolometer ‘pixel’ consists of an absorber attached to a thermistor of resistance R and at a temperature T . The bolometer is weakly coupled to a heat sink at a temperature T_0 , where $T \geq T_0$. Generally, T_0 is referred to as the stage temperature, since when we are making measurements this temperature corresponds to the cold stage of the fridge we are using. In practise there will be a small thermal gradient between what we measure as T_0 and the actual temperature of the heat sink, but this will be too small to be concerned with. The absorber temperature, T , is referred to as the bolometer temperature. The thermal link between the bolometer and the heat sink is of length L and static thermal conductance G_s . The bolometer will have a heat capacity $C(T)$ (it is assumed that the thermal link has zero heat capacity).

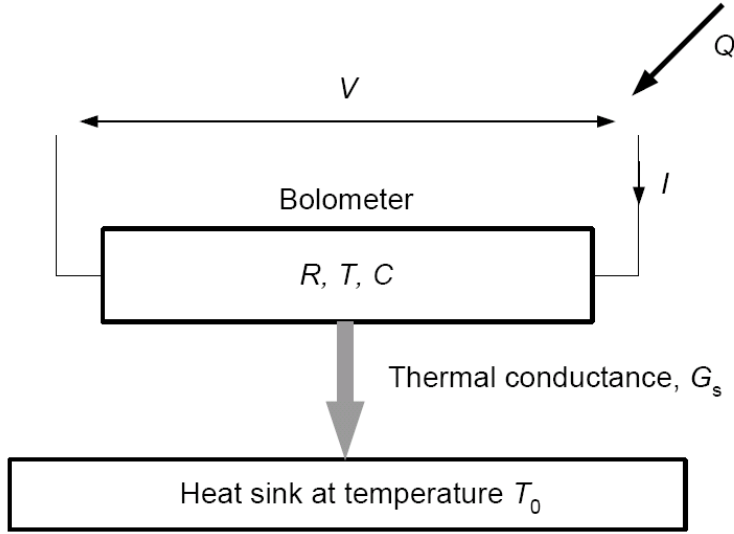


Figure 2: Schematic diagram of a bolometric detector.

The device is read out by measuring the voltage drop across the bolometer. In order to do this, a bias current, I , must be passed through the thermistor, generating a voltage $V = IR$ across it. Figure 3 shows a typical bolometer electrical bias and measuring circuit, with a voltage source V_a providing the bias current to the bolometer, conventionally in series with a load resistance, R_L . The voltage across the bolometer is measured through a low noise voltage amplifier (generally, this will be a cryogenic device to minimise thermal noise in the circuit).

The model described here is that of an ideal bolometer. In practise, this means that the bolometer does not exhibit what are known as ‘non-ohmic’ effects. One example of such an effect is electron-phonon decoupling, in which there is a finite thermal conductance between the electrons and phonons in the thermistor. Although this effect is not fully understood at present, it can be included in our model by treating the two as physically separate components with a thermal conductance that varies as a power law with temperature. The paper by Grannan *et al.* describes an ideal bolometer model that takes these effects, and others, into account. Our model also makes the assumption that power dissipated in the bolometer by the bias current has the same effect as power dissipated by absorbed radiation. This will be true in general, unless electron-phonon decoupling is present (since the electrical power heats the electrons in the thermistor, while the optical power heats the lattice).

Our goal in this model is to be able to reproduce the voltage-current response of the bolometers (known as a load curve). To do this, we need expressions for the resistance of the thermistor element, and the power dissipated in the bolometer. Both of these are functions of the bolometer and stage temperatures.

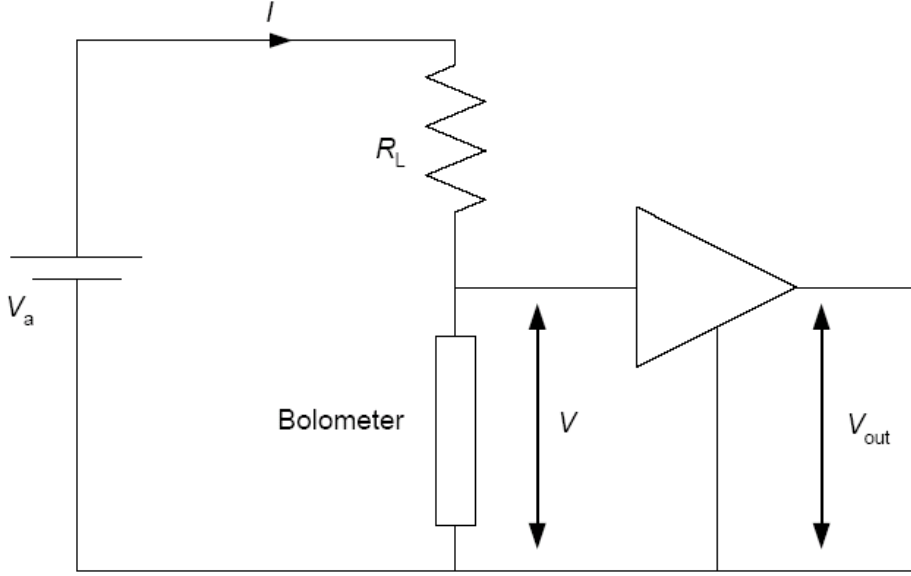


Figure 3: Bolometer bias and measurement circuit.

The total power dissipated in the bolometer, W , is

$$W = P + Q \quad (1)$$

where Q is the absorbed optical power and $P = IV$ is the electrical power due to the bias circuit. The steady state energy balance equation for the bolometer is

$$W = G_s(T - T_0) \quad (2)$$

Some models of ideal bolometer behaviour, such as that of Griffin & Holland, assume that the variation of the conductance of the thermal link with temperature can be expressed as a power law in the form

$$G_s(T, T_0) = G_{s0} \left(\frac{T}{T_0} \right)^\beta \quad (3)$$

where G_{s0} is the thermal conductance at temperature $T = T_0$. In general, this expression is not actually true. Instead, we will make the physically more realistic assumption that it is the variation of the thermal conductivity, k , of the link with temperature that is expressed as a power law:

$$k(T) = k_0 \left(\frac{T}{T_0} \right)^\beta \quad (4)$$

where $k_0 = k(T_0)$. By expressing the thermal conductivity as $k(T)$, we take the variation of thermal conductivity with temperature *across the link* into account, something that is disregarded in some models. This assumption is consistent with the non-equilibrium bolometer theory of Mather, and is that used recently by Sudiwala *et al.* Now, in the steady state

$$W = \frac{\int_{T_0}^T k(t) dt}{\int_0^L \frac{1}{A(x)} dx} \quad (5)$$

where $A(x)$ is the cross-sectional area of the thermal link at position x . With no loss of generality, we can assume that the cross section is constant, $A(x) = A$. Integration of equation (5) then gives

$$W = \frac{A}{L} \frac{k_0 T_0}{(\beta + 1)} (\phi^{\beta+1} - 1) \quad (6)$$

where we have used $\phi = T/T_0$. From equations (2) and (6), we have

$$G_s(\phi) = \frac{A}{L} \frac{k_0}{(\beta + 1)} \left(\frac{\phi^{\beta+1} - 1}{\phi - 1} \right) = \frac{G_{s0}}{(\beta + 1)} \left(\frac{\phi^{\beta+1} - 1}{\phi - 1} \right) \quad (7)$$

where $G_{s0} = k_0(A/L)$. Finally, substituting equation (7) into equation (2), and recalling equation (1), we obtain

$$P(\phi) = \frac{G_{s0} T_0}{(\beta + 1)} (\phi^{\beta+1} - 1) - Q \quad (8)$$

The other parameter that is needed to model the voltage-current characteristics of the bolometer is the variation of the thermistor resistance with temperature, $R(T)$. To be completely general, this should be written as $R(T, V)$ since the resistance of a device varies with both applied voltage *and* temperature. This electric field effect is a further example of the non-ohmic behaviour discussed previously. Again, it is possible to include these effects in the model, but it is generally reasonable to exclude them without compromising the validity of the model. Back to our model, and making this assumption, the resistance of the device therefore only depends on temperature:

$$R(T) = R^* \exp \left[\left(\frac{T_g}{T} \right)^n \right] \quad (9)$$

T_g and n are material parameters, and R^* is a characteristic resistance that depends on both the material and the device geometry.

We are now able to generate the voltage-current characteristic of an ideal bolometer by incrementing T from T_0 to some higher temperature in equations (8) and (9). The electrical power, P and resistance, $R(T)$ can be determined for a given set of values of β , G_{s0} , R^* , T_g , n and radiant power Q . From this, the voltage, V , and current, I , are given by:

$$V = [PR(T)]^{1/2} \quad (10)$$

$$I = \left[\frac{P}{R(T)} \right]^{1/2} \quad (11)$$

The model may be extended to include the dynamic thermal behaviour of the device, which allows other characteristics of the bolometer such as responsivity and the thermal time constant to be determined. The dynamic behaviour of the devices is considerably more complex and goes beyond the scope of this seminar, so we will leave the model at this point. The model is described in full elsewhere, most recently by Sudiwala *et al.*

3 Bolometer Characterisation

In section 2, we have seen that the load curve characteristics of a bolometer can in principle be described by the parameter set β , n , T_g , R^* and G_{s0} , for a given bath temperature, T_0 . To apply this model to a real device, we must be able to determine the values of these parameters by experiment - the process of characterisation. How we carry out this characterisation could be (and nearly was) the subject of a seminar in itself. For anyone interested in how bolometer characterisation is actually carried out, there is a good description of a bolometer test facility included in the paper by Woodcraft *et al.* In this section, we will examine how we apply the model described in section 2 to experimental data.

Before we go any further, it is worth having some feel for the values of the parameters we are discussing. The parameters n , T_g and R^* are dependant on the material used to construct the thermistor element of the bolometer. Modern devices commonly use the material neutron-transmutation-doped germanium:gallium (generally known as NTD-Ge for obvious reasons). It has been found that the value $n = 0.5$ produces good fits to the resistance-temperature variation over the temperature ranges we are generally interested in for this application. Typically, $T_g \approx 15\text{K}$ and $R^* \approx 100 \Omega$ for such thermistor elements. The value of β is dependant on the physical construction of the bolometers. Ideally, $\beta = 1$ for a metallic thermal link and $\beta = 3$ for a crystalline dielectric link; real bolometers may have a mixture of materials with different properties and will exhibit values of β intermediate to these extremes.

Determination of the model parameters require us to accurately control the amount of power dissipated in the bolometer, and to separate the device response to absorbed radiation from that of bias power. There are two main sets of load curve measurements that we must make in order to characterise our bolometer

1. Blanked load curves, voltage current characteristics of the bolometer measured for a variety of bath temperatures, T_0 , ensuring that there is no power loading on the bolometer due to external radiation.
2. Non-blanked load curves, for which the measurements are repeated at various (but not necessarily the same) bath temperatures while viewing a controlled amount of external radiation. The incident power would be provided by a black body source at a known temperature and an appropriate filter system to restrict the radiation to the desired passband and a representative intensity.

In the following discussion of how we use the load curve data, we will primarily restrict ourselves to consideration of blanked load curves. It should be clear in the few instances when this is not the case. The principles described in the rest of this seminar can straightforwardly be extend to non-blanked data, although incident power does complicate the issue.

Model fitting to a single load curve

At first glance, it may seem that we can determine all of the necessary parameters to characterise our bolometer from a single load curve. However, we can show that, in reality, this is not the case. One possible way in which we can compare our model to experimental data is to express the measured load curve as R versus P . If we assume that $n = 0.5$, then from equations (8) and (9)

$$\ln \left[-R \frac{dP}{dR} \right] = -(2\beta + 3) \ln \left[\ln \left[\frac{R}{R^*} \right] \right] + \ln \left[\frac{2G_{s0}T_g^{\beta+1}}{T_0^\beta} \right] \quad (12)$$

For the purposes of this exercise, we will assume that we know the stage temperature, T_0 , to sufficient accuracy (this is unlikely to be the case). Equation (12) is linear in $\ln[\ln(R/R^*)]$, with gradient $-(2\beta + 3)$ and intercept $\ln[2G_{s0}T_g^{\beta+1}/T_0^\beta]$, but only for the correct value of R^* . A graph of χ^2 against R^* from a linear least-squares fit would allow us to determine R^* and β . This is illustrated in figure 4 for a synthetic load curve generated from a parameter set of nominal values, of particular relevance being $R^* = 100 \Omega$.

The derivative was determined numerically from the synthetic data by differentiation of an interpolation function of the R vs. P curve, as would be done for real data. The optimum recovered value for R^* is found from the minimum of the interpolated $\chi^2 - R^*$ curve, as shown in figure 4a. The recovered value from this curve is 100Ω , as we would expect. Substituting this value of R^* into equation (12) allows us to make a linear least-squares fit (shown in figure 4b). The gradient of this fit gives us β directly. For a blanked load curve, in the limit $P \rightarrow 0$, the bolometer temperature $T \rightarrow T_0$ and $R(T, P \rightarrow 0) = R(T_0)$ (or more commonly R_0 , the *zero bias resistance*). This can be determined from the R - P curve, and substituted into equation (9) to deduce T_g . G_{s0} can then be found from the intercept of the least-squares fit and using our value of T_g . Applying this to the synthetic curves recovers the other model parameters initially used to generate the data - as expected.

In practice, equation (12) is difficult to apply since it requires extremely low-noise data. Figures 5 and 6 show the same fitting process for synthetic load curves, but with noise added to the voltage and current values at the 0.01% and 0.1% noise levels respectively. It can be seen from figures 5a and 6a that incorrect values of R^* are recovered, resulting in noisy plots. It has been shown from synthetic data that a load curve must be measured to better than 0.05% in order to fit equation (12) with any confidence. This level of accuracy in measurement is not practically achievable.

Non-linear fitting to load curves

Since we cannot fit our model with any reliability to a single load curve, we need an alternative method of parameter derivation. This is possible by measuring a “family” of load curves over a range of bath temperatures (and ultimately radiant powers), and then using a *non-linear* fit method for our model parameters. We can combine equations (8) and (9) into a form suitable for non-linear curve fitting:

$$P(R) = X \left[\left(\frac{T_g}{T_0 \ln \left(\frac{R}{R^*} \right)^n} \right)^Y - 1 \right] - Q \quad (13)$$

where $Y = \beta + 1$ and

$$X = \frac{G_{s0} T_0}{Y} \quad (14)$$

We cannot simply fit X , Y , T_g and Q to measured load curves and expect sensible results to be determined. The problem is compounded by the fact that we will frequently want to fit T_0 as a free parameter to the data - although it would appear the T_0 should be determined directly from our test setup, in practise experimental and calibration errors force us to treat the bath temperature as another fit parameter. The reason we cannot make a fit of equation (13) to our data is that the parameters are not actually independent. For example, in blanked load curves, T_0 is a function of T_g , R_0 and R^* :

$$T_0 = \frac{T_g}{\ln \left(\frac{R_0}{R^*} \right)^n} \quad (15)$$

where R_0 is the thermistor resistance at zero bias current. Similarly, for non-blanked load curves, Q can be expressed as a function of the other parameters. Furthermore the best fit parameter values are not unique. It can be shown that, in some cases, best fit curves for equation (13) can be reproduced exactly by parameter sets with negative values of thermal conductance and radiant power. Such parameter sets are completely non-physical.

Clearly, we need a method to break this degeneracy. Fortunately, we can determine some of the parameters in the model using a set of blanked load curves, thus reducing the number of free parameters in the non-linear fit.

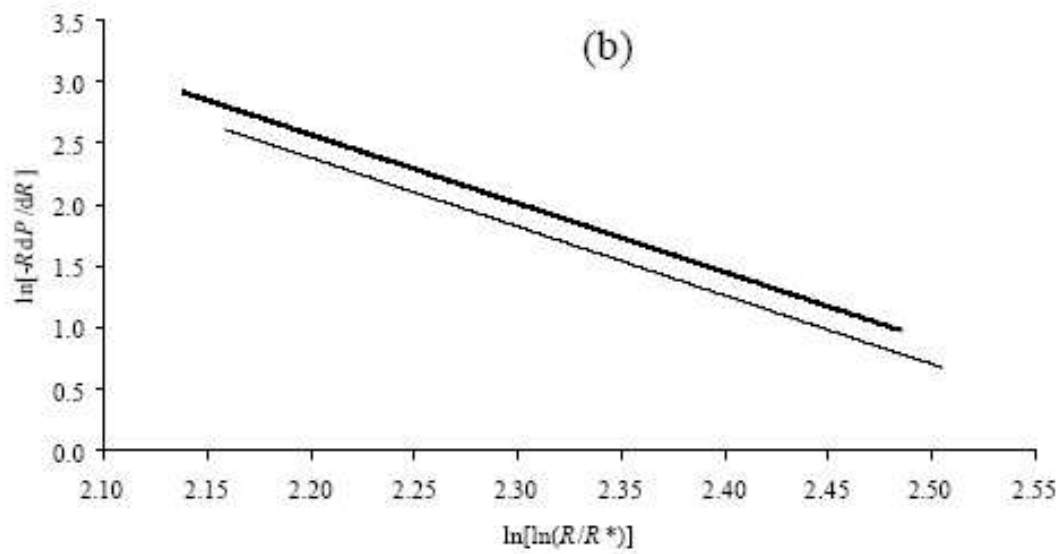
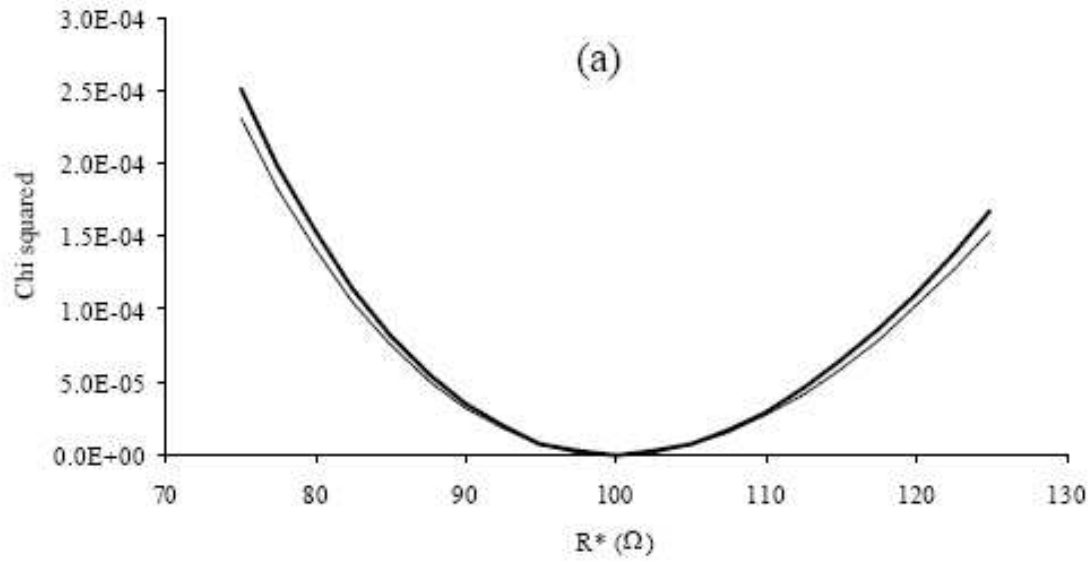


Figure 4: (a) χ^2 against R^* fits to equation (12) for synthetic load curve data. (b) The load curve data plotted according to equation (12) for the “best” value of $R^* = 100 \Omega$ from (a). In both cases, the lighter line represents blanked data ($Q = 0$) and the heavier line non-blanked data (Sudiwala *et al.*).

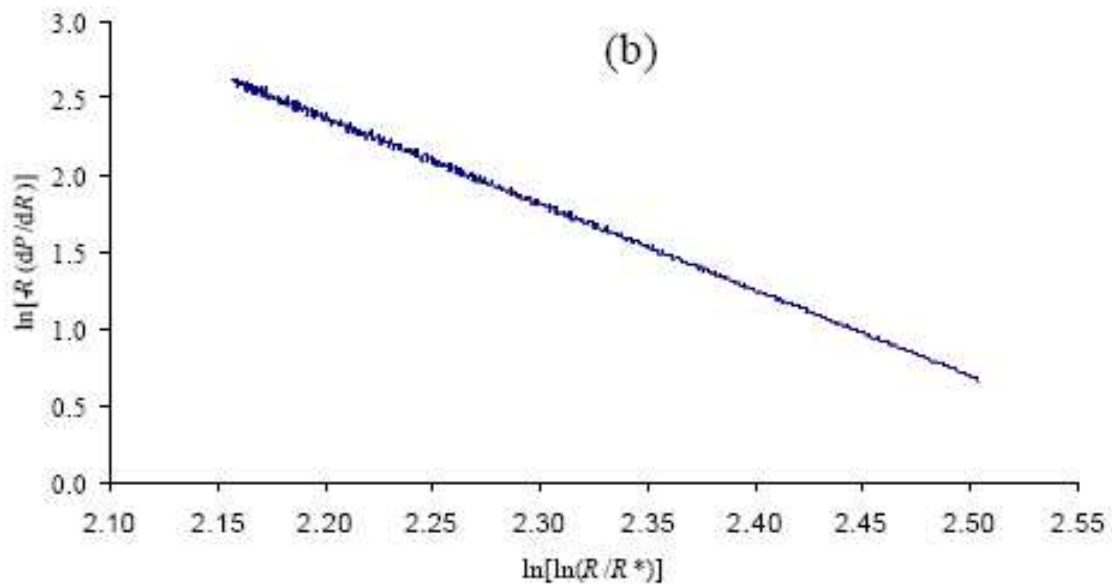
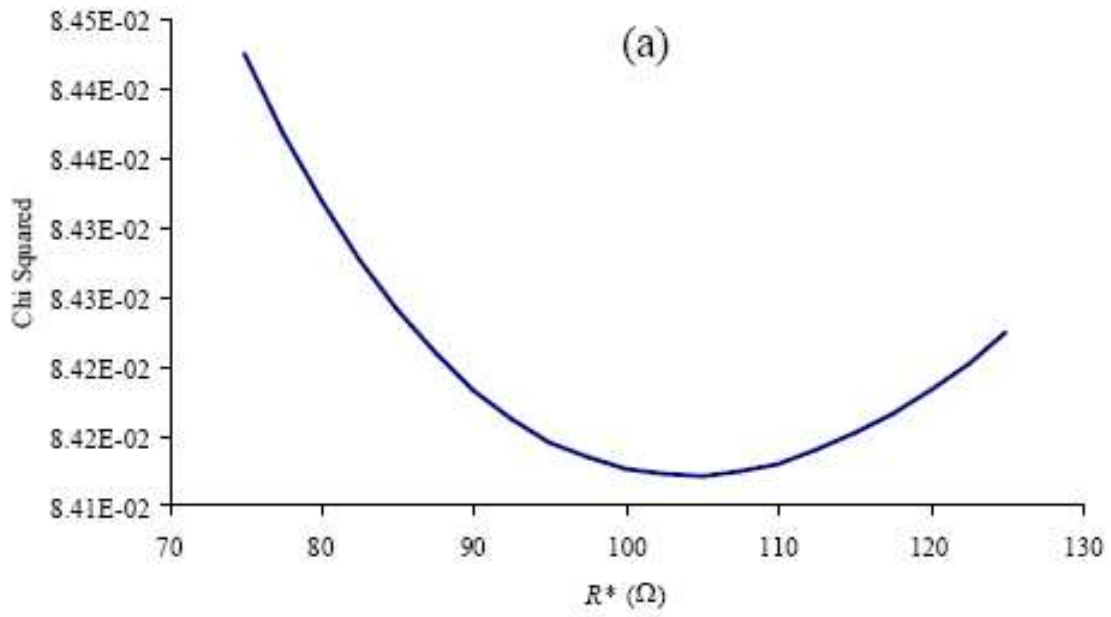


Figure 5: (a) χ^2 against R^* fits to equation (12) for synthetic load curve data with 0.01% added noise. The “best” value of $R^* = 103.5 \Omega$ (b) The load curve data plotted according to equation (12) for the value of R^* from (a) (Sudiwala *et al.*).

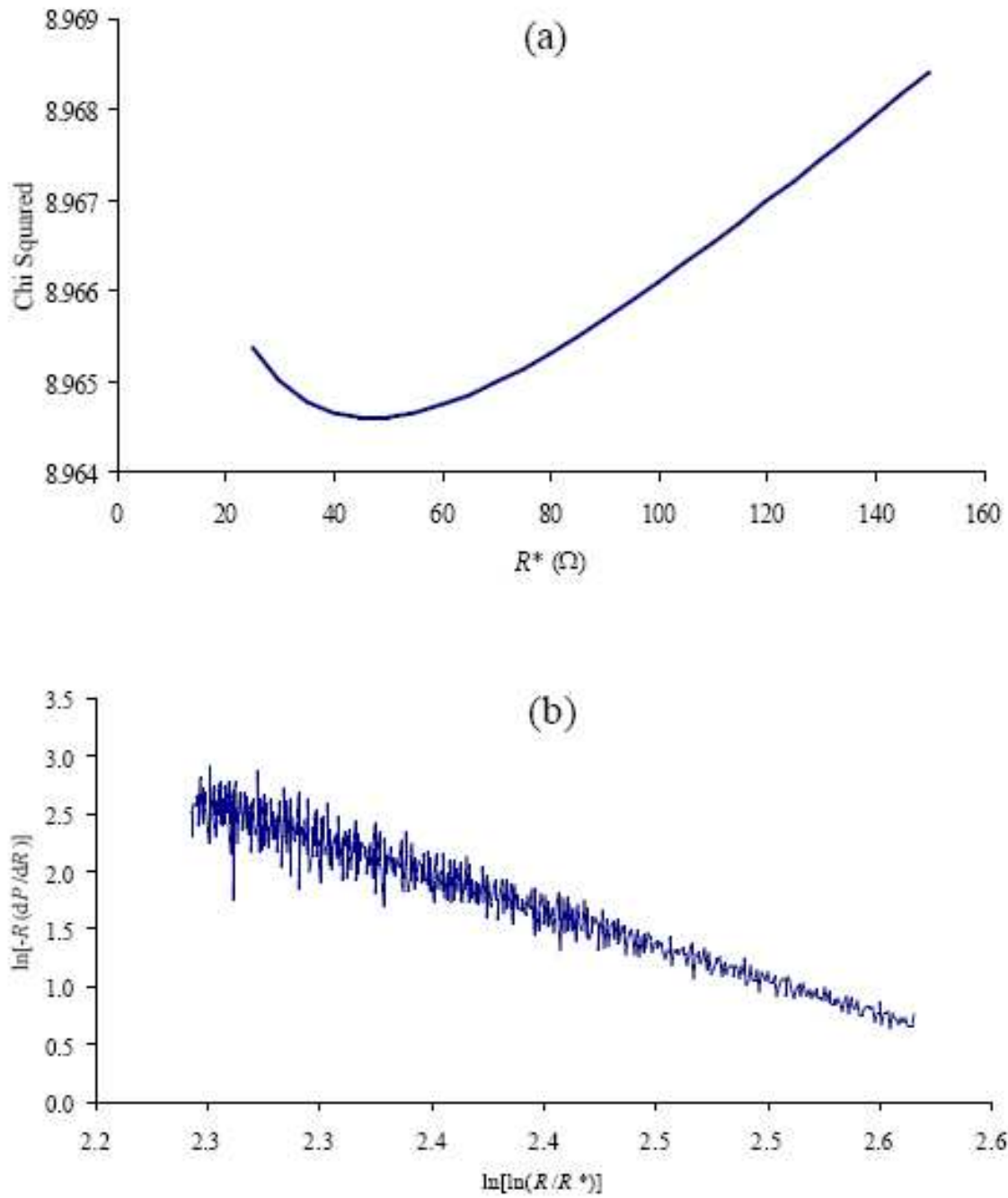


Figure 6: (a) χ^2 against R^* fits to equation (12) for synthetic load curve data with 0.1% added noise. The “best” value of $R^* = 47 \Omega$ (b) The load curve data plotted according to equation (12) for the value of R^* from (a) (Sudiwala *et al.*).

Two-step model fitting to load curve “families”

The most common method for determining the parameters of the thermal model from experimental data uses a two stage approach. The first step is to determine $R(T)$ from equation (9). Our load curves plot V as a function of the bias current, I , so we can obtain R from the gradient of the curves. However, there is a slight problem. Figure 7 shows an example family of load curves for a prototype bolometer from the high-frequency instrument on the Planck Surveyor CMB mission at a range of stage temperatures. We can clearly see from this that the gradient of the curves is not constant, and is negative in some regions of the curve. The reason for this inconsistency is that as the bias current increases, self-heating in the thermistor reduces the resistance. This effect does complicate operation of the bolometer, but in terms of characterisation we simply have to use the start of each load curve where the resistance is constant (the value of R in this region is R_0).

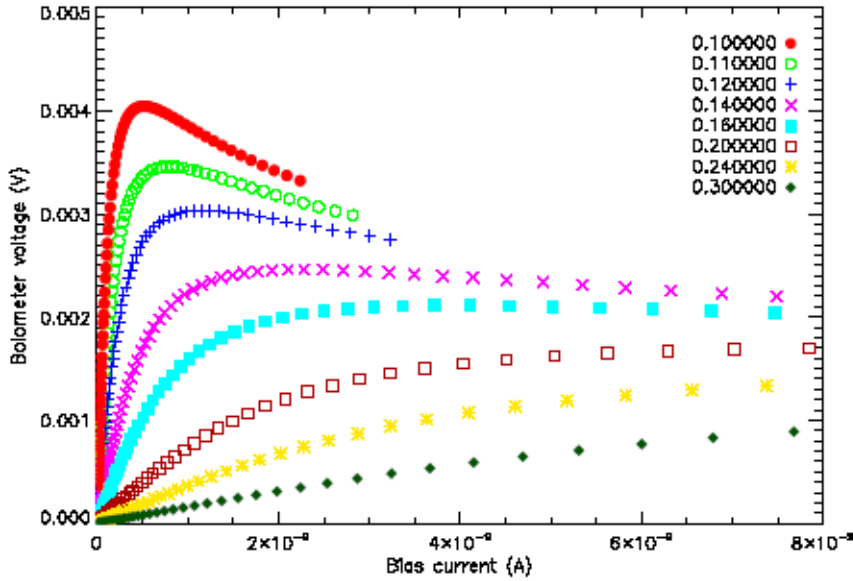


Figure 7: Example bolometer load curve measurements. Different symbols correspond to different stage temperatures between 100 and 300 mK, as indicated in the legend.

It is a matter of judgement as to how much of the load curve to use before the resistance deviates from a constant gradient, but one way to simplify this is to plot $R = V/I$ against I on a log-log scale, as shown in figure 8. The point where the load curve deviates from a straight line is considerably more obvious when plotted in this way.

We can now plot the zero bias resistance as a function of temperature. From equation (9), for the case where $T = T_0$, we can write that

$$\ln(R_0) = \ln(R^*) + \left(\frac{T_g}{T_0}\right)^n \quad (16)$$

A plot in the form $\ln(R_0)$ as a function of $1/\sqrt{T_0}$ will be linear (figure 9), assuming that $n = 0.5$ as discussed previously, with the gradient and intercept of a linear fit yielding T_g and R^* . If n differs from 0.5, then an examination of the fit residuals from a linear fit will tell us as such. The solution to this problem would be to carry out a non-linear fit with n as an additional free parameter.

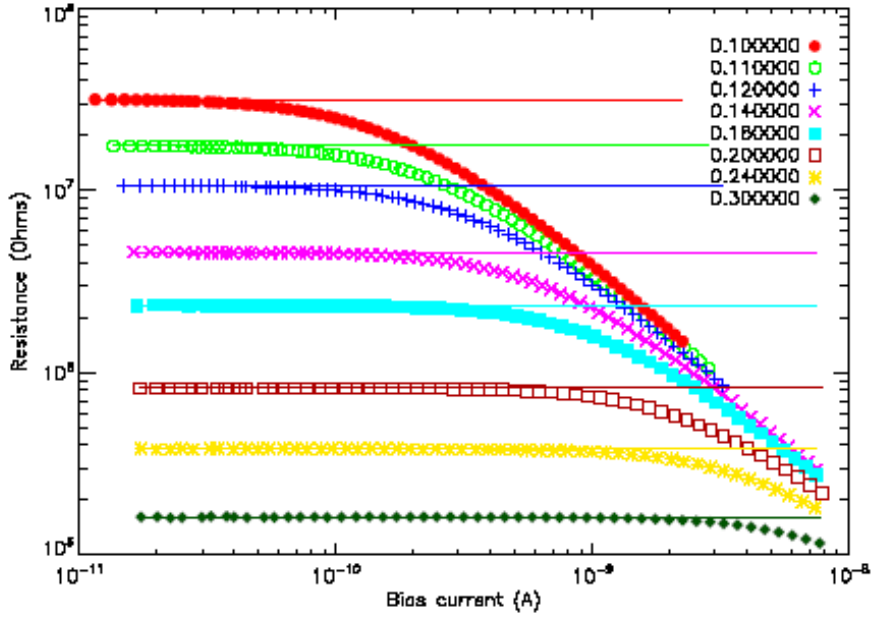


Figure 8: Load curves from figure 7, plotted as bias current against resistance. The solid lines indicate the chosen value for the zero bias resistance, R_0 .

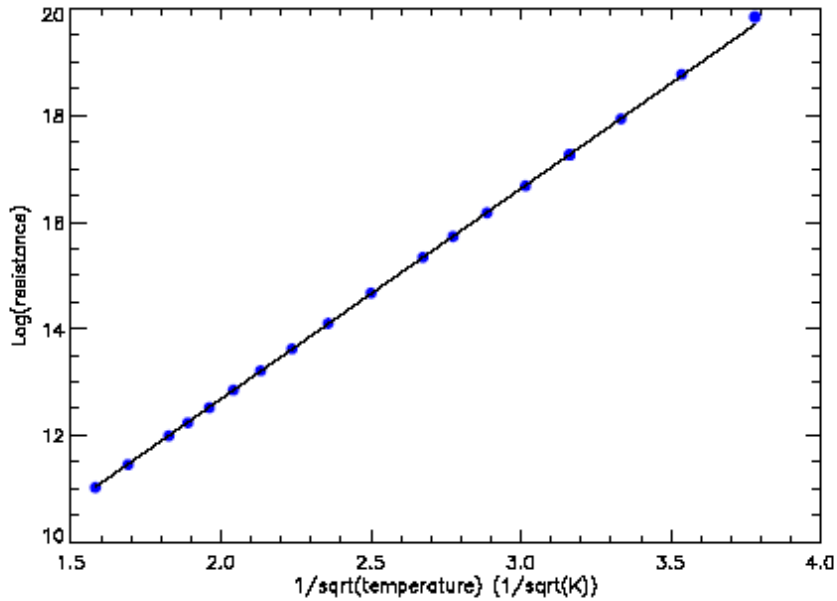


Figure 9: Plot of bolometer zero bias resistance as a function of temperature, with a linear fit of the form of equation (16).

Very small departures of linearity from a plot such as that in figure 9 will also result if the bolometer absorbs any stray power, even if our value of n is correct. Such stray power can be caused by a radiation leak in the experimental setup, or by microphonic, electrical or RF pickup. To illustrate this effect, figure 10 shows a plot of $\ln(R_0)$ vs. $1/\sqrt{T_0}$ from synthetic data for blanked data, and with small values of absorbed power Q included to simulate stray power loading on the bolometer.

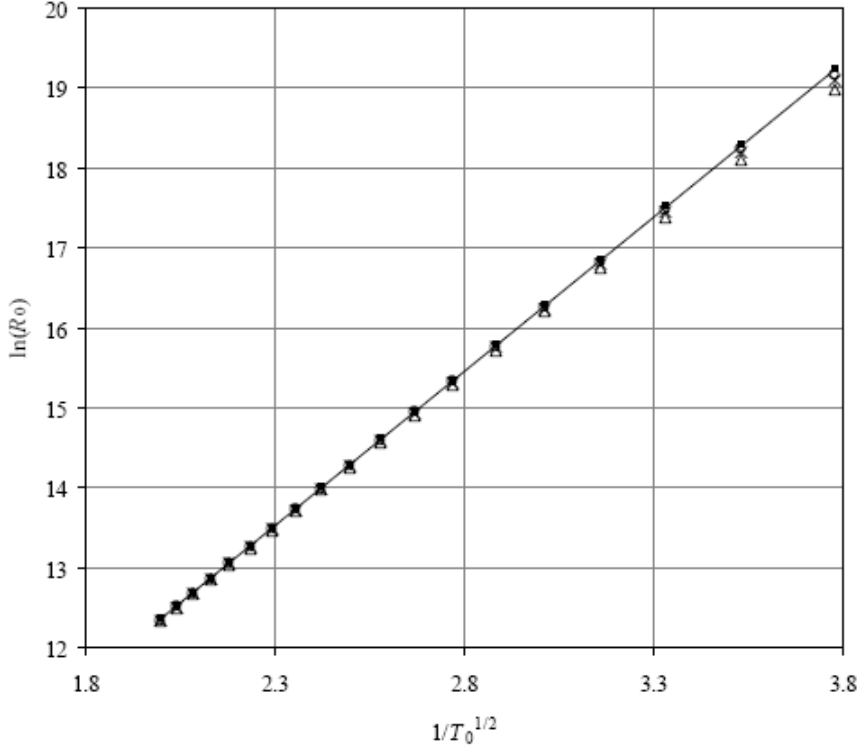


Figure 10: $\ln(R_0)$ vs. $1/\sqrt{T_0}$ curves from synthetic load curves: blanked (solid squares); stray radiant power $Q = 0.05$ pW (open diamonds), 0.1 pW (crosses) and 0.2 pW (open triangles). The line is fitted to the blanked data points (Sudiwala *et al.*).

Now that we have determined R^* , T_g , and confirmed that our value of n is suitable, we can return to the non-linear fit in equation (13) to determine G_{s0} and β . An alternative approach is to determine these parameters directly by looking at changes in T as the bias current is increased, in a similar way to how any thermal conductance would be experimentally determined. Whichever method we use, we should now be able to apply the parameters we have determined to predict the behaviour of our bolometer at an arbitrary stage temperature. An obvious check at this stage would be to attempt to predict the load curves we have already measured from our model. Figure 11 shows plots of the same load curves as in figure 7, but with fits from the thermal model included. As can be seen, there is generally very good agreement. If there is any significant deviation between the fits and the measured data, then the likely culprits are non-linear effects in the bolometer behaviour. These effects are most likely to be a problem at low stage temperatures, generally $T_0 < 100$ mK.

The role of non-blanked load curves

While blanked load curves in principle allow us to determine all of the parameters in the thermal model presented in section 2, non-blanked load curves are also important to fully characterise our bolometer. Although we have not discussed this aspect of bolometer characterisation, ultimately the bolometer will be exposed to external radiation, and there are a number of parameters, such as the dynamic response of the devices to an ac optical load, that can only be determined from non-blanked measurements.

Over and above this, non-blanked data provide the possibility of a number of internal consistency checks for the experimental data. Examples of these are that the values of β and G_{s0} should be the same for blanked and non-blanked load curves recorded at the same bath temperature, and that the value of Q should be the same for all non-blanked load curves within a family recorded at the same source temperature.

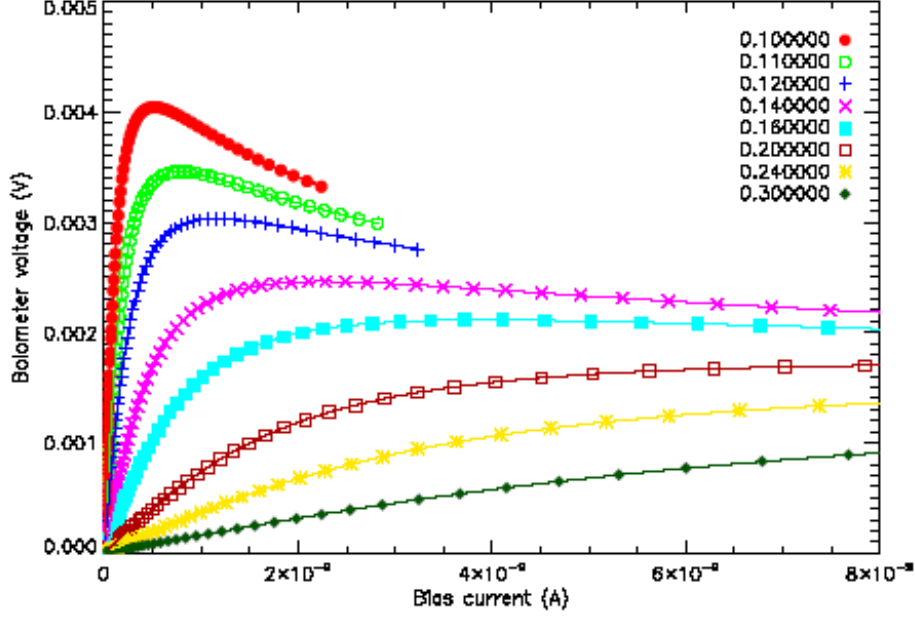


Figure 11: Bolometer load curves from figure 7 including model fits.

Applying the model to arbitrary values of T_0

There is one rather obvious problem with applying our model parameters to the bolometer at stage temperatures other than those we have measured. While β , n , T_g and R^* are not functions of temperature, G_{s0} will change as the stage temperature changes. The solution to this actually comes from equation (3). At the time we said that it was incorrect to assume that the variation of static thermal conductance with temperature obeyed a power law of this form because no account was taken of the variation of thermal conductivity across the link as the temperature of the link varied from T to T_0 . However, there is one special case where $k(T)$ will be constant - when $T = T_0$. Therefore, if we change the stage temperature from T_0 to some other temperature T'_0 , it can be shown that

$$G_{s0}(T'_0) = G_{s0}(T_0) \left(\frac{T'_0}{T_0} \right)^\beta \quad (17)$$

Just to reiterate, this relationship is only true for the static thermal conductance at $T = T_0$ - not for an arbitrary value of T .

4 Conclusion

During the course of this seminar, we have described a simple model of an ideal bolometric detector that would allow us to predict the basic static behaviour of a bolometer, and which could be extended to consider the more complex dynamic behaviour of the device. We have considered what data we need and how we can use that data to obtain the parameters in the model, so allowing us to predict the behaviour of the bolometer under arbitrary conditions for which we have no direct measurements from our experiments. We have also briefly considered some of the problems of obtaining data from real devices, and some of the problems of fitting our model to the data. There are a great number of practical considerations when it comes to obtaining and analysing the experimental data described so far which we have not discussed - the interested party should look to the references listed below for more detailed discussions

of the experimental and modelling procedures (in particular the recent works of Sudiwala *et al.* and Woodcraft *et al.*).

It is hoped that this seminar has provided a brief introduction to the ideas of modelling and characterising bolometric detectors, and has given an idea of how important such work actually is. In short, unless we have a detailed understanding of how a detector behaves, we can't use it!

References

- Grannan, S. M., Richards, P. L., and Hase, M. K.: 1997, *International Journal of Infrared and Millimeter Waves* **18**, 319
- Griffin, M. J. and Holland, W. S.: 1988, *International Journal of Infrared and Millimeter Waves* **9**, 861
- Holland, W., Duncan, W., and Griffin, M.: 2002, in S. Stanimirovic, D. Altschuler, P. Goldsmith, and C. Salter (eds.), *ASP Conf. Ser. 278: Single-Dish Radio Astronomy: Techniques and Applications*, pp 463–491
- Mather, J. C.: 1982, *Appl. Opt.* **21**, 1125
- Mather, J. C.: 1984, *Appl. Opt.* **23**, 584
- Sudiwala, R. V., Griffin, M. J., and Woodcraft, A. L.: 2002, *International Journal of Infrared and Millimeter Waves* **23**, 545
- Woodcraft, A. L., Sudiwala, R. V., Griffin, M. J., Wakui, E., Maffei, B., Tucker, C. E., Haynes, C. V., Gannaway, F., Ade, P. A. R., Bock, J. J., Turner, A. D., Sethuraman, S., and Beeman, J. W.: 2002, *International Journal of Infrared and Millimeter Waves* **23**, 575